Journal of Water Process Engineering 33 (2020) 100991

Contents lists available at ScienceDirect

Journal of Water Process Engineering

journal homepage: www.elsevier.com/locate/jwpe

Zeolite-A deposited on glass hollow fiber for forward osmosis applications

Siti Nurfatin Nadhirah Mohd Makhtar[a], Norfazilah Muhammad[a], Mukhlis A. Rahman[a,*], Khairul Hamimah Abas[b], Azian Abd Aziz[c], Mohd Nazri Mohd Sokri[a], Mohd Hafiz Dzarfan Othman[a], Juhana Jaafar[a]

[a] Advanced Membrane Technology Research Centre (AMTEC), Universiti Teknologi Malaysia, 81310 Skudai, Johor, Malaysia
[b] Faculty of Electrical Engineering, Universiti Teknologi Malaysia, 81310 Skudai, Johor, Malaysia
[c] Language Academy, Universiti Teknologi Malaysia, 81310 Skudai, Johor, Malaysia

ARTICLE INFO

Keywords:
Zeolite membrane
Glass hollow fiber
Forward osmosis
In situ hydrothermal synthesis

ABSTRACT

This work investigated the effects of reactant concentrations and synthesis periods on in situ deposition of zeolite membranes on glass hollow fibers. The separation performances of the zeolite membranes in forward osmosis applications were studied based on pure water fluxes and reverse solutes. The reactant concentration of 0.66 M enabled zeolite membrane deposited onto glass hollow fiber to give a water flux of 4.50 L m^{-2} hr^{-1} with reverse solute of 0.05 kg m^{-2} hr^{-1}. When the deposition time was reduced to 12 h and 18 h, water fluxes increased to 62.25 and 71.92 L m^{-2} hr^{-1}, respectively.

1. Introduction

Recovery of fresh water from seas and oceans has been regarded as an alternative option to minimize water scarcity as they cover most of the Earth's surface, comprising approximately 97% [1]. Various technologies have been used in desalination processes, such as ion exchange, electrodialysis and distillations [1,2], with attention shifting to membrane technology using the reverse osmosis process to harvest fresh water in a large scale. However, reverse osmosis is an energy-intensive technology, which is linked to greenhouse gas (GHG) emissions and other negative environmental impact such as organism impingement and brine disposal at the outfall [3]. As an alternative to the reverse osmosis process, forward osmosis (FO) has been considered to be a promising approach to water purification in overcoming challenges in water recovery. The FO process utilizes an osmotic pressure gradient through a semipermeable membrane as a basic process in water purification. The osmotic pressure gradient, which is the driving force in the FO operation, occurs when a semipermeable membrane is placed between a solution of high concentration (draw) and a solution of lower concentration (feed). Although FO can be a solution for hydraulic pressure-driven membrane processes, it is not a substitute for reverse osmosis (RO) [4].

Polymeric membranes have been utilized extensively for FO processes. However, the disadvantages of polymeric membranes, i.e. biofouling, oxidation, metal oxide fouling, abrasion and mineral scaling due to their low stability, have caused ceramic membranes to receive greater attention as FO membranes [5]. This is due to the advantages of the ceramic materials themselves such as resistance to mechanical, chemical and thermal stress, high porosity and hydrophilic surface, which is suitable for water treatment applications [6]. Nevertheless, it should be noted that not all ceramic materials can be used as membrane materials for FO applications. This is because conventional ceramic materials, i.e. alumina and zirconia, have limited pore structures, resulting in such materials to lack the capability to effectively remove salt from water. It is thus suggested that micro-porous ceramic membranes, i.e. zeolite, be used as a material for the preparation of FO membranes.

As a ceramic membrane, zeolite has gained attention as it has been proven to improve water treatment in terms of hydrophilicity, surface charge, porosity, antimicrobial properties, permeability and solute rejection [7]. Thus, zeolite is considered a promising ceramic material to be applied in seawater desalination. The hydrophilic nature of zeolite due to the presence of silanol (SiOH) groups on its surface can render the membranes to have better resistance to biofouling [8]. In addition, zeolite membranes have been proven to have superior performance for ion removal from aqueous solutions by reverse osmosis (RO) processes which indirectly fit the FO processes [9]. Zeolite is frequently impregnated as a thin layer on polyamide membranes to improve water fluxes without large losses of salt rejection [7,8,10]. Jamali et al. reported that zeolite nanosheet is a potential membrane for desalination as long as the pore sizes of the zeolite are smaller than 5.5 Å, thereby possessing a larger channel density for water permeation, with cages size shell diameter of 6.5 Å for salt rejection [9]. The main mechanism

* Corresponding author.
E-mail address: r-mukhlis@utm.my (M.A. Rahman).

https://doi.org/10.1016/j.jwpe.2019.100991
Received 4 April 2019; Received in revised form 26 September 2019; Accepted 6 October 2019
Available online 24 October 2019

of the separation/solute rejection is the size exclusion of hydrated ions and electrostatic repulsion (Donnan exclusion) at the intercrystalline pore entrance [11].

The synthesis of zeolite has played a significant role in zeolite development since the past decade [9]. Zeolite is usually synthesized using hydrothermal crystallization, in situ hydrothermal synthesis, vapor phase transport, a sol-gel method, chemical growth, galvanic metal deposition, leakage-blocked method and microwave synthesis [12–15]. Commonly, in situ hydrothermal approach will construct a thin dense layer of zeolite membrane, becoming a very appropriate membrane for seawater desalination [12]. Parameters involving temperature, reaction time and molar composition (concentration) in the zeolite synthesis will affect the performance of zeolites. Therefore, this study aimed at preparing zeolite membranes by hydrothermal synthesis onto a glass hollow fiber. The unique properties of glass fiber encompassing flexible geometric form and pore structure, chemical inertness, optical transparency, high mechanical and thermal stability and reactive surface, have resulted in glass membranes to be used in a wide range of applications [16,17]. These advantages have made glass fiber a suitable support for zeolite membranes. The phase inversion and sintering technique were adopted in preparing porous glass hollow fiber for the deposition of zeolite membranes. This process enabled the porous glass hollow fiber to be produced in the simplest way, compared to the conventional technique of glass membrane fabrication [18]. In this work, various parameters in preparing zeolite membranes were investigated, namely, synthesis duration and total molar concentration of reactants. Effects of these parameters on the physical and chemical properties of zeolites were correlated with the membranes' performance in terms of water flux and reverse solute.

2. Experiments

2.1. Materials

Zeolite (5A) was purchased from Sigma Aldrich, USA and used as a starting material. The powder was dried at 60 °C for 24 h before use. Commercially available yttria-stabilized zirconia (YSZ) powder with particle size of 0.3 μm (d_{50} = 0.3 μm) was purchased from Fuel Cell Material and used as the ceramic particles mixed with the zeolite. Radel A300 polyethersulfone (PESf) was provided by Ameco Performance, USA. Polyethyleneglycol 30-dipolyhydroxystrearate, (Arlacel P135) was purchased from CRODA Inc. N-methylpyrrolidone (NMP) was purchased from QREC, New Zealand. Sodium aluminate (Na_2AlO_3) and sodium trisilicate ($Na_2O_7Si_3$) was purchased from Sigma Aldrich as alumina and silica sources, respectively. Sodium hydroxide (NaOH) was purchased from Emsure, Darmstadt, Germany. All chemicals were used as received without further treatment.

2.2. Preparation of glass hollow fiber

Porous glass membranes were prepared using the phase inversion based spinning technique following our previous method [18]. 1 wt.% of Arlacel P135 was dissolved gradually in NMP solution before the addition of zeolite (30 wt.%) and zirconia (20 wt.%) particles. Later, the suspension was rolled with different sizes of alumina agate milling balls (20 mm and 10 mm) in a planetary ball-milling machine (NQM-2 Planetary Ball Mill). The process was continued for another 48 h after the addition of a polymer binder at a specific ratio of zeolite, YSZ, and polymer. Tap water was used as both internal and external coagulants. The extrusion rate and air gap were fixed at 10 mL min^{-1} and 15 cm, respectively. The hollow fiber precursor was further immersed in tap water for 24 h to complete the phase inversion process.

The hollow fiber precursors were then sintered in a tubular furnace (XY-1700, China). The sintering temperature was first increased at a rate of 3 °C min^{-1} to 400 °C where the thermolysis process, a process where the polymer binder is removed, was carried out for 1 h. The temperature was further increased to 800 °C at 4 °C min^{-1}, held for 2 h. At this stage, the polymer binder would have been burnt-off, leaving only the zeolite material. The final sintering temperature was fixed at 1000°C with a rate 5°C min^{-1} and held for 8 h to allow the ceramic particles to combine, becoming bigger grains. Finally, the temperature was cooled down to room temperature at a rate 5°C min^{-1}.

Table 1
Composition of zeolite NaA synthesis solutions.

Concentration (M)	Synthesis composition (molar ratio)			
	Silicon	Aluminum	Sodium	Water
0.113	10	5	15	5000
0.221	10	5	15	3000
0.664	10	5	15	1000

2.3. Synthesis of zeolite using in situ hydrothermal technique

Zeolite was prepared by dissolving sodium hydroxide (NaOH) in distilled water and divided into two equal volumes. Sodium aluminate and sodium trisilicate were dissolved in NaOH solutions, separately. The formed silica solutions were poured drop-wise into a sodium aluminate solution while stirring vigorously. The final solutions were then poured into a Teflon-bottle containing glass hollow fibers as zeolite support. The hydrothermal process was carried out by placing the Teflon-bottle in an oven at 120 °C for 24 h. When this process was completed, the membrane was washed with distilled water and dried. The molar ratio of the zeolite solution composition is shown in Table 1.

2.4. Membrane performance measurements

Fig. 1 depicts the lab-scale forward osmosis (FO) system. The membrane was capped by epoxy at both ends without closing the membrane lumen. A draw solution was prepared by dissolving NaCl in deionized water. NaCl was chosen as it is easily characterized by osmotic pressure and diffusion coefficient [19]. The concentration of NaCl as the draw solution was fixed at 100,000 ppm. Crosscurrent mode was used as the feed solution (FS) and together with the draw solution (DS) were flowed in a closed loop separately. The FS was flowed on the active layer of the membrane while the DS was flowed into the membrane lumen. Variable speed peristaltic pumps (New Era Pump, Inc) were used to pump the liquids, with the difference in liquid mass weighted using a weighing balance (Smith).

Water flux was measured by weighing the change in the FS over a selected period. Mass of the DS increased as water from the FS

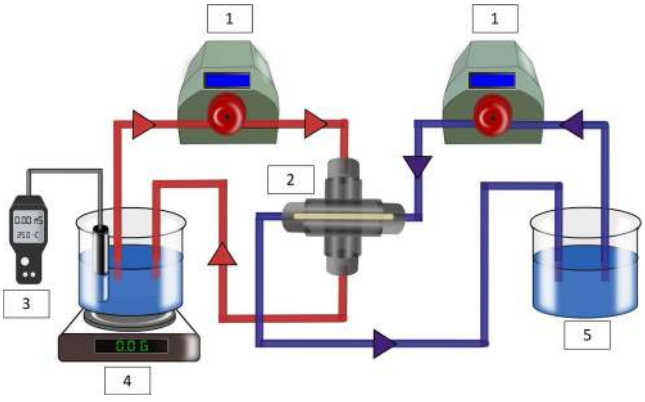

Fig. 1. Schematic diagram of the laboratory-scale FO system that consists of peristaltic pump (1), hollow fiber membrane cell (2), ion conductivity meter functioning as a thermometer (3), electronic weighing balance with feed solution (4), and draw solution (5).

permeated across the membrane due to osmotic difference. The water flux was calculated using Eq. (2):

$$J_W = \frac{V}{t \times A} \quad (2)$$

where, J_W (L. m^{-2}.hr^{-1}) is water flux, V is the volume of the permeability based on the mass change and density (L) (V(L) = mass (kg) / density (ρ)), t is time (s) and A is the total effective membrane area (m^2). Reverse solute of NaCl was determined by measuring conductivity of DS and FS using a conductivity meter (Eutech Cond 6+, Thermo Scientific, Singapore) before and after FO filtration. The reverse solute was calculated using Eq. (3) [20]:

$$Js = f\frac{(Vt.Ct)}{Am\,\Delta t} \quad (3)$$

where, J_s (kg. m^{-2}.h^{-1}) is reverse solute, V is the volume of the permeability based on the mass change and density (L) (V(L) = mass (kg) / density (ρ)), C is the NaCl concentration (kg L^{-1}), t is time (s) and A is the total effective membrane area (m^2). All of the performances were repeated three times using membranes selected from a same batch.

The structure parameter (S) and the tortuosity factor (τ) were used to evaluate the concentration polarization phenomenon and calculated using Eq. (4) [21,22]

$$S = \frac{l\tau}{\varepsilon} \quad (4)$$

where, l (μm) is the total membrane thickness and Ɛ is the total porosity of the FO membrane.

2.5. Characterizations

Zeolite membranes were characterized using the X-ray diffraction (XRD), field emission scanning electron microscopy (FESEM) and nitrogen adsorption-desorption isotherms. The cross-sectional images of the zeolite membranes were obtained using the FESEM (Zeiss CrossBeam 340). The membranes were snapped into 3 mm length and placed on a metal holder. The FESEM samples were coated with gold/platinum mixture under vacuum for 3 min. at 20 mA. X-ray diffraction (XRD) analyses of the membrane were carried out using Philips PW1710 at scan rate 1°/s, ranging from 4° to 80°. The membrane sample was finely grounded and mounted on a special plat holder prior to analysis. Nitrogen adsorption-desorption isotherms were obtained using BET characterization (Micromeritics Autopore IV). The samples were degassed for 5 h at 350 °C over night under vacuum condition prior to the measurement. The pore volume and pore size distribution of the zeolite samples were acquired using the Barret-Joyner-Halenda (BJH) model.

3. Results and discussion

3.1. Preparation of glass hollow fiber for zeolite deposition

Glass hollow fiber was prepared using a zeolite suspension that was spun in a coagulation bath at an extrusion rate of 10 mL min^{-1}, bore fluid of 9 mL min^{-1}, and air gap of 15 cm. The hollow fiber precursors were later sintered at 1000 °C for 8 h to transform the zeolite particles into glass [18]. The cross-sectional image of the glass hollow fiber was acquired using the SEM analysis as shown in Fig. 2a. YSZ particles dispersed uniformly throughout the glass hollow fiber membrane. It can be seen that the hollow fiber has an asymmetric membrane, containing sponge-like and finger-like voids. This was due to water, used as a coagulant, trapped in the cross-section during the phase inversion process. Fig. 2b shows the FTIR spectra for the glass hollow fiber. The peaks at 713 and 972 cm^{-1} denoted the vibration of overlapping symmetric and asymmetric of T−O bond, where T is Si or Al, while the peaks at 1362 and 1515 cm^{-1} denoted the YSZ peaks. This analysis confirmed the absence of chemical bonds between YSZ particles and glass. Fig. 2c shows the XRD spectrum of the glass hollow fiber ranging from 4 to 75° of the Bragss's angles (2θ). The results indicated that the glass hollow fiber has an amorphous phase. The peaks at 30°, 50° and 60° represented the YSZ, whereas the peak at 34° represent the Al_2O_3. The presence of Al_2O_3, which was a by-product formed due to zeolite sintering, indicated a complete transformation of zeolite to the glass phase [18,23–26].

3.2. Effects of reactant concentration of the deposition of zeolite membrane onto glass hollow Fiber

Zeolite membranes were prepared using three different reactant concentrations at 120 °C for 24 h, namely 0.13 M, 0.22 M and 0.66 M, respectively. The atomic ratios between sodium, aluminum and silicon for all these reactants were kept constant. The purpose for the variation in the reactant concentrations was to study the deposition characteristics of zeolite membranes on glass hollow fiber. The XRD analysis confirmed that zeolite-A membranes prepared using different concentrations were successfully synthesized, as shown in Fig. 3. Zeolite membranes synthesized using the reactant concentration of 0.66 M had the highest number of zeolite XRD peaks. However, the number of these peaks was reduced when the concentration was reduced to 0.13 M. This trend was due to the fact that the formation of zeolite crystals was influenced by the supersaturation in the zeolite gel, which was dependent on the water content. When the amount of water increased, the supersaturation process, which is typically followed by nucleation and crystal growth, decelerated. This will eventually slow the formation of the zeolite. This process was completely halted when supersaturation did not occur [27,28].

The FESEM analysis was used to study the deposition of zeolite membranes on glass hollow fiber. The results are shown in Figs. 4 and 5. At lower magnification, the cross-sectional images show the absence of any thick layer of zeolite on the outer surface of the glass support. When zoomed at higher magnification, the images show the presence of bulk particles on the cross section of the glass hollow fiber. Fig. 4c(iii) shows particles deposited onto glass hollow fiber having a zeolite signature shape, which was also dispersed into the macro-void of the support. Fig. 5 shows the FESEM images of the outer surface of glass hollow fibers, fully deposited with zeolite membranes. Variations in the shape of the zeolite grains with different reactant concentrations can be seen in Fig. 5a(iii)–c(iii). As proved by the XRD results in Fig. 3, the zeolite grains synthesized using the lowest reactant concentration did not possess a cubical crystal shape, which marks the shape of zeolite NaA. In contrast, cubical shaped zeolites can be clearly observed using FESEM when the reactant concentration was increased to 0.66 M. The figure shows the zeolite membranes remained deposited on the glass surface even after a rigorous cleaning with water during post treatment and harsh preparation of the FESEM analysis. The glass hollow fiber is believed to be an excellent support for zeolite growth as the glass has an active surface hydroxyl group, namely −OH [29,30]. A strong interaction between the zeolite membrane and glass hollow fiber could be formed due to intermolecular forces of hydrogen bonds and lone pair attractions. Hydrogen bond is formed through surface hydroxyl groups of both materials, whereas lone pair attractions occur due to the interaction between oxygen ions in both zeolite and glass. This explains the existence of lone pairs developing between oxygen ions in −OH groups and Na^+ in zeolite.

N_2 physisorption analysis was carried out on the zeolite samples to determine their BET specific surface area and total pore volume. Table 2 represents the textural properties of the zeolite NaA particles synthesized at reactant concentrations ranging from 0.13 M to 0.66 M. The results showed that the zeolite membranes synthesized in this work had low specific surface areas, ranging from 2.32 to 14.38 m^2. g^{-1}, and low total pore volumes, ranging from 0.016 to 0.129 cm^3. g^{-1}. Typically, zeolite has been known to possess high surface area, but porous materials with a low specific surface and low total pore volume may be

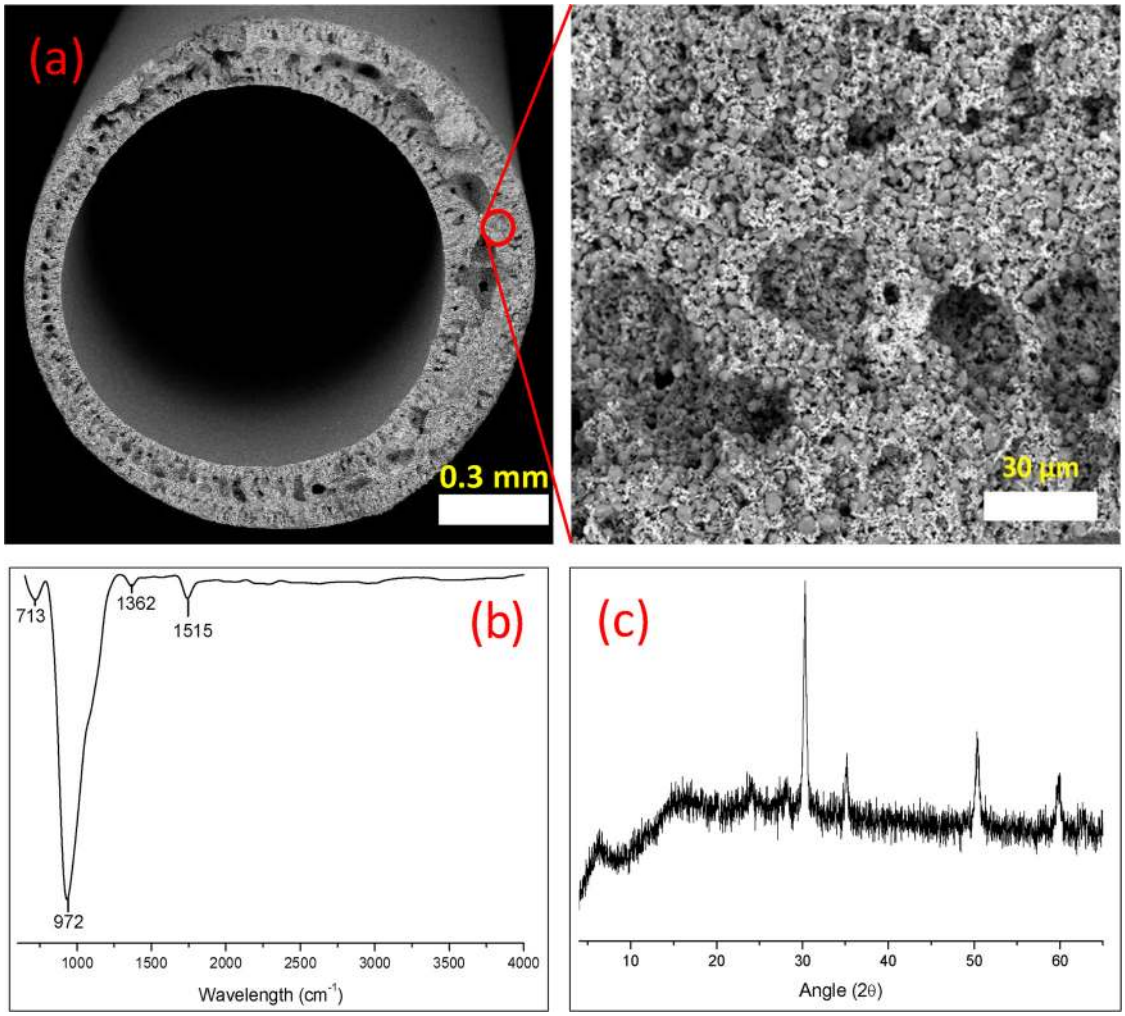

Fig. 2. (a) Cross-sectional image, (b) ex-situ infrared spectra, and (c) diffraction spectrum of glass hollow fiber prepared using a zeolite suspension through the phase inversion and sintering process.

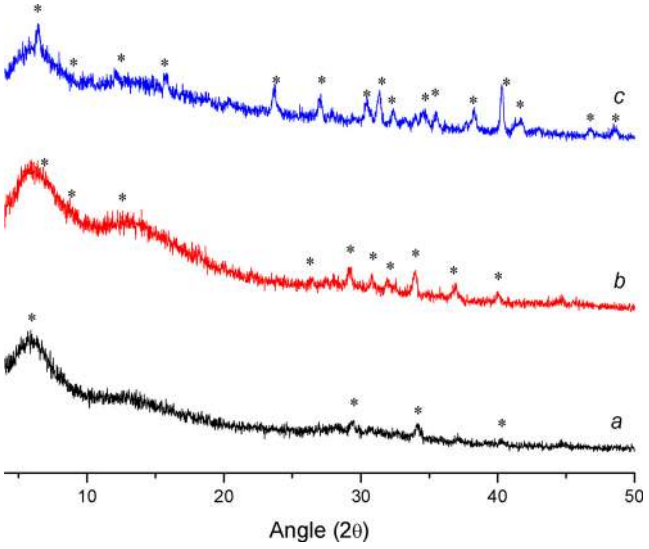

Fig. 3. XRD spectra of zeolite particles synthesized using different reactant concentrations of (a) 0.13 M, (b) 0.22 M, and (c) 0.66 M, at synthesis temperature of 120 °C. The symbol * denotes the peaks of the zeolite.

contributed by the synthesis condition. At high synthesis temperature, i.e. 120 °C, there was a reduction in the water content, as water evaporated into the vapor phase. This phenomenon caused a reduction in the size of the intra-crystalline porosity [27,31,32]. Among the three samples, the highest specific surface area was achieved by the zeolite membrane prepared using the reactant concentration of 0.22 M (14.38 $cm^3.g^{-1}$) with the highest total pore volume of 0.129 $cm^3.g^{-1}$. The range of pore size was determined using an isotherm graph and BJH pore size distribution.

N_2 physisorption analysis was carried out to identify the presence of mesoporosity in zeolite membranes using N_2 adsorption/desorption isotherms and BJH mesopore size distribution, as shown in Figs. 6 and 7. Fig. 6 demonstrated the N_2 adsorption/desorption isotherms of zeolite membranes synthesized at different reactant concentrations. The figure shows that all zeolite samples adsorbed insignificant amount of N_2, represented by P/P_0 ranging from 0.0 to 0.3. This can be correlated with the absence of micropores in the zeolite membranes. The figure shows that zeolite membranes prepared using various reactant concentrations have isotherms with hysteresis loop. However, the hysteresis loop of P/P_0 started at 0.6 and became significant above 0.9, indicating that the zeolite membranes had limited mesoporous structures. The result also showed that the agglomeration of zeolite occurred during the synthesis process, especially the zeolite prepared using a reactant concentration of 0.13 M. This condition was represented by the significant N_2 adsorption when $P/P_0 > 0.9$. Agglomeration caused the formation of macro pores, which enabled significant adsorption of N_2 during the N_2 adsorption/desorption analysis.

BJH pore size distribution of zeolite membranes prepared using

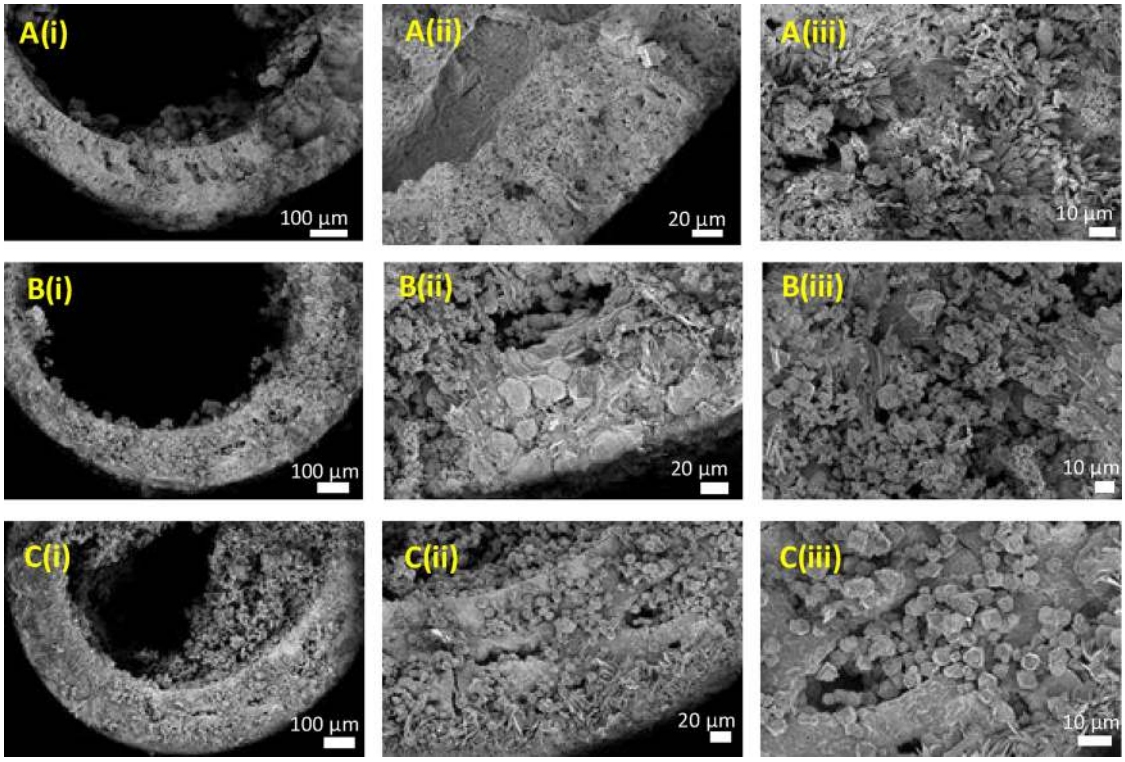

Fig. 4. Cross-sectional FESEM images of zeolite membranes deposited onto glass hollow fiber, at different magnifications, prepared using reactant concentrations of (A) 0.13 M, (B) 0.22 M and (C) 0.66 M, at synthesis temperature of 120 °C.

various reactant concentrations are shown in Fig. 7. The figures suggest that the zeolite membranes prepared in this work had a wide pore size ranging from 2 to 120 nm. This result supports the finding discussed in Fig. 6 that predicted macroporous structure with pore size > 50 nm would be formed due to agglomeration of zeolite. The results also showed that all samples had a hierarchical characteristic [33], indicating the formation of uneven particle sizes. This might give the zeolite membrane a mesoporous characteristic as different grain sizes

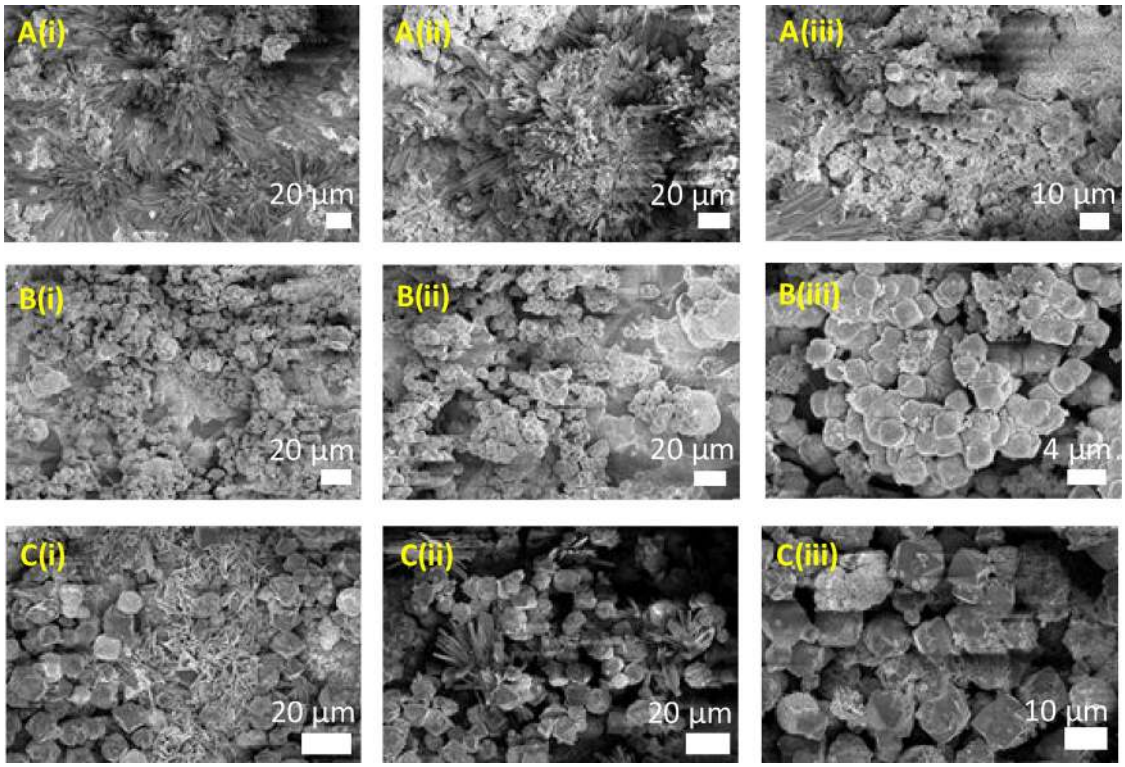

Fig. 5. FESEM images of the outer surface of the zeolite membranes at different spots, prepared using reactant concentrations of (A) 0.13 M, (B) 0.22 M and (C) 0.66 M, at synthesis temperature of 120 °C.

Table 2
Textural properties of zeolite membranes synthesized using reactant concentrations of 0.13 M, 0.22 M and 0.66 M, at synthesis temperature of 120 °C.

Reactant Concentrations	[a]Sbet	[b]V_{total}
0.13 M	7.1017	0.021
0.22 M	14.3767	0.129
0.66 M	2.3253	0.016

[a] Sbet: Bet specific surface area ($m^2 g^{-1}$).
[b] V_{total}: total pore volume ($cm^3 g^{-1}$).

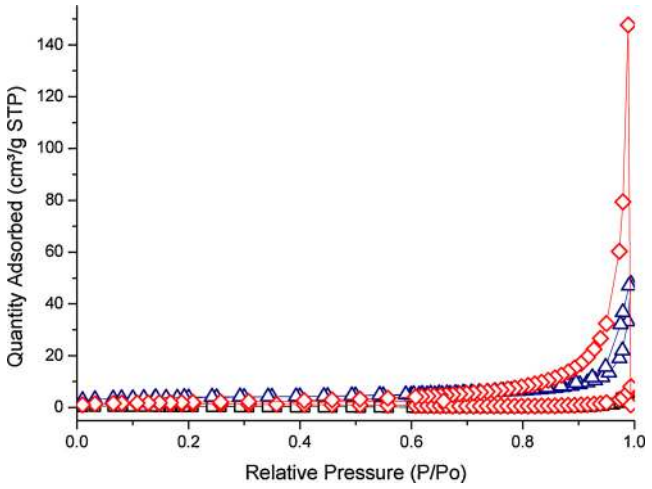

Fig. 6. N_2 adsorption/desorption isotherms of zeolite particles synthesized using reactant concentrations of 0.13 M (○), 0.22 M (△) and 0.66 M (□), at synthesis temperature of 120 °C.

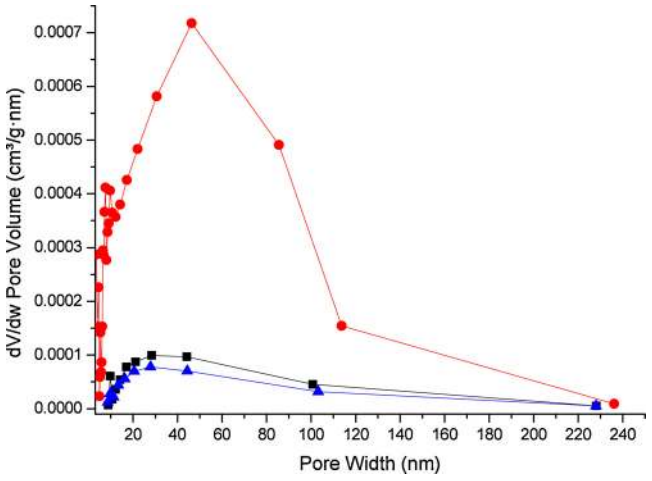

Fig. 7. BJH pore size distribution derived from isotherm adsorption branch for zeolite membranes prepared using reactant concentration of 0.13 M (■), 0.22 M (●), and 0.66 M (▲), at synthesis temperature of 120 °C.

had created a tangible gap between the zeolite grains.

3.3. Effects of in situ synthesis period on the deposition of zeolite membrane on glass hollow fiber

To study the effect of the synthesis period on the deposition of zeolite membranes on glass hollow fiber, this parameter was varied, ranging from 3 h to 24 h, using the reactant concentration of 0.66 M. Fig. 8 shows the FESEM images of the cross-section and outer surface of zeolite membrane prepared using various synthesis periods. It can be seen that zeolite membranes with a cubical A-type characteristic, were deposited on the glass hollow fiber for all samples. Zeolite membranes prepared for 3 h was not able to be deposited uniformly on the outer surface of the glass hollow fiber due to limited time for the deposition process. When the synthesis period was increased, the deposition process of the zeolite membrane improved. It can be seen by the formation of a complete and continuous layer of zeolite prepared using 12, 18 and 24 h synthesis time. However, zeolite membrane synthesized for 24 h was too dense, which may inhibit water diffusion, thus reducing permeability during the separation process. The FESEM images also show that the zeolite membrane prepared using in situ hydrothermal synthesis was able to grow firmly on the glass support as a thin membrane layer. However, the mechanism of zeolite deposited onto an inert support is complex, which involves a number of reaction steps i.e. molecular self-organization, nucleation, aggregation, crystallization, and growth. The combination of these reaction steps in an in situ synthesis of zeolite is indeed a challenge, particularly in obtaining the desired properties of the zeolite membrane [34]. A similar phenomenon occurred when the zeolite was synthesized on the glass fiber. The FESEM images showed that zeolite membranes grew uncontrollably in both the outer surface and in the lumen of the glass fiber.

To study the crystallinity of the prepared zeolite membranes using different synthesis periods, the XRD analysis was performed on all membrane samples. The results are shown in Fig. 9. The results showed that zeolite membranes prepared using a synthesis period of 3 and 6 h were in the amorphous form, whereas zeolite membranes prepared using a synthesis period ranging from 12 to 24 h were in the crystalline form. This implied that an increase in the reaction time would enhance the crystallinity of the zeolite membrane. Zeolite membranes synthesized for 12 h had a characteristic of zeolite NaA, indicating this was the minimum synthesis period required in order to obtain this characteristic. When the synthesis period was extended to 24 h, diffraction peaks of the zeolite particles changed, giving a different trend compared to zeolite particles prepared for 12 and 18 h, with new XRD peaks appearing, representing the formation of zeolite NaX. However, zeolite NaA still appeared on this sample, based on the zeolite database included in the XRD analysis, represented by (▲). It is expected that NaA zeolite may exist as NaX zeolite when the synthesis time was prolonged [35].

To study the porosity of zeolite membranes prepared under various synthesis time, N_2 physisorption analysis was carried out on all samples to determine their BET specific surface area and total pore volume. Table 3 shows the textural properties of the zeolite NaA prepared ranging from 3 to 24 h. The results showed that all samples had low specific surface area and total pore volume, except for samples prepared using the synthesis period of 12 and 18 h. Zeolite particles synthesized for 12 and 18 h had a specific surface area of 181.10 $m^2 g^{-1}$ and 134.62 $m^2 g^{-1}$, respectively. Both samples also showed a significant total pore volume of 0.106 $m^2 g^{-1}$ and 0.084 $cm^3 g^{-1}$, respectively. An increase in the specific surface areas of zeolite membranes prepared with this range can be associated with the synthesis condition. To obtain a high surface of zeolite NaA, various studies suggested that the synthesis process should be carried out at a synthesis temperature of 100 °C for 24 h. However, in this work, the synthesis temperature was increased to 120 °C, which was expected to enhance the zeolite deposition process onto the glass hollow fiber. An increase in the temperature should be compensated with the reduction of synthesis time. Therefore, a reduction in synthesis time from 12 h to 18 h may be an ideal duration for zeolite with high surface area to be produced. Further reduction in the synthesis time, ranging from 3 h to 6 h caused a reduction in the surface area of the zeolite particles, causing the formation of premature zeolites as proven by the XRD analysis.

Fig.10 shows the N_2 adsorption/desorption isotherms analysis for zeolite particles prepared using different synthesis times. Zeolite particles synthesized for 3 to 18 h displayed isotherms with hysteresis loop. The hysteresis loop resulted from a specific pore in zeolite membranes that were filled with N_2 at high pressures and emptied at low pressures.

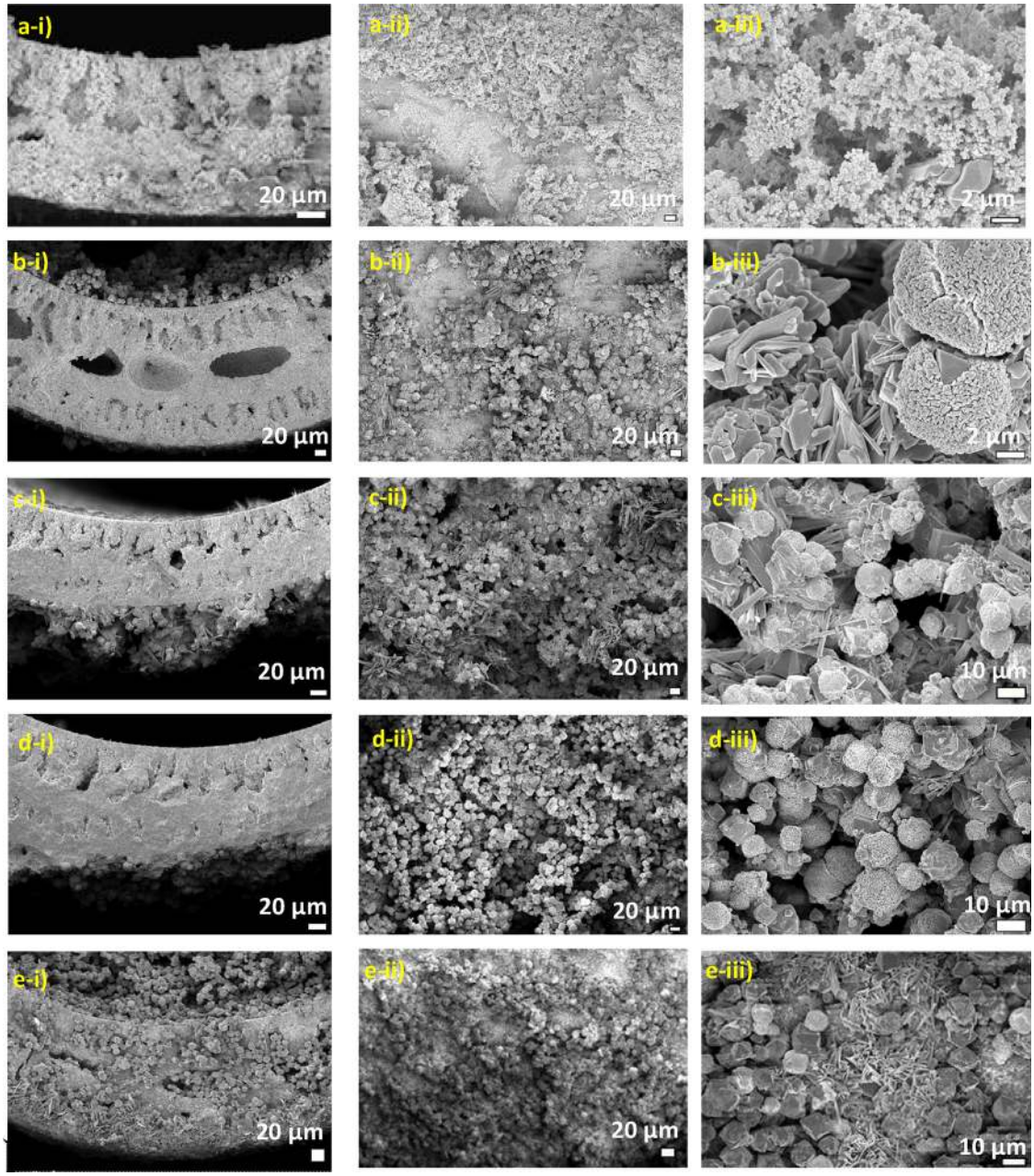

Fig. 8. FESEM images of the zeolite membranes prepared for (a) 3 h, (b) 6 h, (c) 12 h, (d) 18 h and (e) 24 h at synthesis temperature of 120 °C. The samples were magnified at (i) 300 x magnification (cross-section (i), 200 x magnification (outer surface) (ii) and magnification ranging from 800 x to 5000 x (outer surface).

Zeolite membranes synthesized for 3 h, 6 h and 24 h respectively, were found to have N_2 insignificant adsorption, compared to zeolite membranes synthesized for 12 h and 18 h. The results showed that zeolite membranes synthesized ranging from 12 h to 18 h had both microporous and mesoporous structures, as these samples possessed high N_2 adsorption at $P/P_0 < 0.2$ and $0.2 < P/P_0 < 1.0$, respectively. High N_2 adsorption of both regions enabled the zeolite membranes to possess high surface area as shown in Table 3. To study the pore size distribution of the zeolite membranes at the mesoporous region, BJH mesopore size analysis was carried out for all zeolite membranes synthesized at different synthesis times. The figure shows that the zeolite membranes synthesized for 12 h and 18 h have similar pore size distributions ranging from 5 nm to 40 nm, while zeolite membranes prepared for 6 h and 24 h have insignificant pore size distributions ranging from 10 nm to 50 nm. Absence of the mesopore structure in these membranes was proved by N_2 adsorption/desorption isotherms in Fig. 10. However, zeolite membranes synthesized for 3 h showed significant pore size distribution similar to the zeolite membranes synthesized ranging from 12 h to 18 h. Referring to Fig. 10, the membranes possessed high N_2 adsorption $P/P_0 > 0.8$, indicating existence of the mesoporous structure in the samples. Although this membrane has been categorized as premature zeolites, using XRD analysis in Fig. 9, agglomeration of particles was expected to occur during the synthesis process. It is expected that this condition may lead to the formation of mesoporous structures.

3.4. Performance of zeolite membranes on glass hollow fibers for salt removal

The performance of zeolite membranes deposited on glass hollow fiber synthesized using various reactant concentrations and synthesis periods were evaluated based on the membranes' water fluxes and

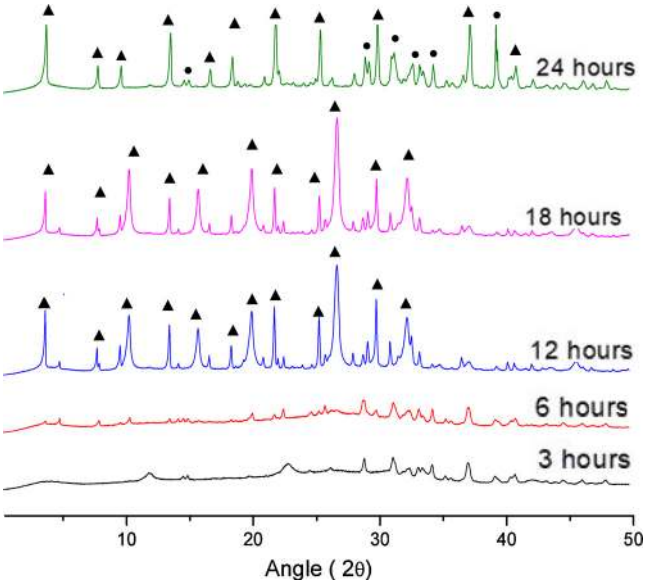

Fig. 9. XRD diffraction pattern of zeolite synthesis in an autogenous pressure at 120 °C at different reaction time for 0.66 M zeolite concentration, NaA zeolite (▲), NaX zeolite (●).

Table 3
Textural properties of zeolite particles synthesized using reactant concentration of 0.66 M for various periods ranging from 3 to.24 h

Synthesis period (hr)	[a]Sbet	[b]V_{total}
3	5.47	0.046
6	6.39	0.020
12	181.10	0.106
18	134.62	0.084
24	2.33	0.016

[a] Sbet: BET specific surface area ($m^2. g^{-1}$).
[b] V_{total}: total pore volume ($cm^3. g^{-1}$).

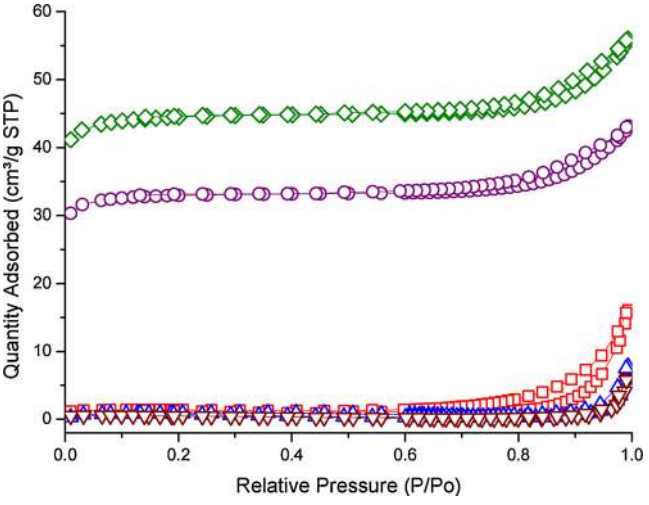

Fig. 10. N_2 adsorption/desorption isotherms for zeolite particles prepared using 0.66 M reactant concentration for (□) 3 h, (△) 6 h, (◇) 12 h, (○) 18 h, and (▽).24 h .

rejections. In this work, a performance study was carried out using the forward osmosis system, which required a draw solution to be introduced in the lumen and feed solution to be introduced on the outer surface of the membrane. Water fluxes were categorized as either positive (+ve) fluxes or negative (-ve) fluxes, based on the membrane characteristics. Positive fluxes referred to the flow of water from dilute solution/pure water to the concentrated solution, following a natural phenomenon called the osmosis process. Negative fluxes refer to the flow of the draw solution, which has a high solute concentration to feed solution, with a negligible solute concentration. However, this condition was undesirable as the membranes used for the separation process contained defects that prevented the occurrence of the osmosis process from the feed solute to the draw solute [36,37]. In this work, NaCl solution (100,000 ppm) was used as the draw solution whereas DI water was used as the feed solution.

Table 4
Water fluxes and reverse solute fluxes of zeolite membranes prepared using various reactant concentrations. The osmosis process was governed by 100,000 ppm sodium chloride (NaCl) solution used as draw solute.

Concentration (M)	Water Fluxes ($L\ m^{-2}h^{-1}$)	Reverse solute ($kg\ m^{-2}h^{-1}$)
0.00	−600.00 ± 1.78	511.97 ± 1.56
0.13	−124.75 ± 6.01	302.69 ± 5.01
0.22	−248.62 ± 2.55	32.55 ± 2.98
0.66	4.50 ± 2.79	0.05 ± 0.029

Table 4 shows the water fluxes and reverse solute fluxes of zeolite membranes prepared using reactant concentrations of 0.13, 0.22 and 0.66 M via in situ hydrothermal process. A separation process was also carried out using bare glass hollow fiber in order to compare the performance of zeolite membranes in rejecting salt. The bare glass hollow fiber showed a water flux and a reverse solute of -600.00 $L.m^{-2}h^{-1}$ and 511.97 $kg\ m^{-2}h^{-1}$, respectively. These readings indicated that bare glass hollow fiber should not be used as a membrane for desalination. Although glass hollow fibers deposited with zeolite membranes prepared using reactant concentrations of 0.13 and 0.22 M showed improvements in terms of water fluxes and reverse solutes, these improvements were still insufficient for efficient desalination. This inefficiency is probably due to the zeolite membranes not being deposited uniformly on the glass hollow, causing defects that halted the osmosis process. The various concentrations used were not sufficient in producing defect-free zeolite membranes. When the reactant concentration was increased to 0.66 M, the osmosis process started to occur which gave a positive flow of 4.50 $L.m^{-2}h^{-1}$ with reverse solute of 0.05 $kg\ m^{-2}h^{-1}$. It is expected that within the synthesis period of 24 h, the surface of glass hollow fiber would be fully deposited with zeolite membrane, resulting in the absence of any defects and enabling osmosis to occur.

To study the optimum period of depositing zeolite membranes on glass hollow fiber, the synthesis period was varied ranging from 3 h to 24 h. This range was based on studies carried out by Okamoto et al. [38], and Bayati et al. [39]. Okamoto et al. stated that the shortest reaction time to prepare NaA zeolites via single step crystallization was 3 h [38], while Bayati et al proposed a maximum time of 24 h for preparing zeolite [39]. The performance of zeolite membranes in performing forward osmosis is listed in Table 5. When in situ deposition time was reduced to 12 h and 18 h, water fluxes increased to 62.25 to

Table 5
Water fluxes, reverse solutes and S value of zeolite membranes prepared using various synthesis period. The osmosis process was governed by 100,000 ppm sodium chloride (NaCl) solution used as draw solute.

Crystallization time (hr)	Water fluxes ($L\ m^{-2}\ h^{-1}$)	Reverse solute ($kg\ m^{-2}h^{-1}$)	S value (μm)
3	−4.61 ± 1.35	136.49 ± 1.55	–
6	51.72 ± 1.39	45.99 ± 1.25	7.8135
12	62.25 ± 1.20	0.11 ± 0.0148	4.5556
18	71.92 ± 0.09	0.05 ± 0.019	4.8684
24	4.50 ± 2.79	0.05 ± 0.029	23.2913

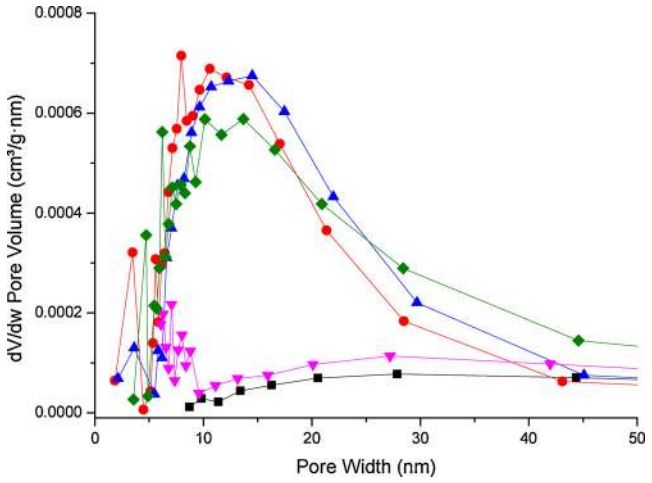

Fig. 11. BJH pore size distribution of zeolite particles synthesized for 3 h (●), 6 h (▼), 12 h (▲), 18 h, (●) and 24 (■).

71.92 L.m^{-2} h^{-1}, respectively. Reverse solutes for zeolite membranes in situ deposited for 12 h and 18 h were 0.11 kg m^{-2} h^{-1} and 0.05 kg m^{-2} h^{-1}, respectively. Improvements in the separation performance can be correlated with porosity of the membrane. Both samples showed significant surface area and porosity to enable zeolite in facilitating the diffusion of water through its framework but halting high reverse solute to occur. Although zeolite membranes deposited in situ for 24 h had a positive flux, the water flux was low. Surprisingly, the membrane had an insignificant surface area and porosity, as shown in Table 3 and Fig. 11. When the deposition period was reduced to 6 h, reverse solute increased significantly. The membrane enabled the osmosis process to occur, but it was too thin to resist any reverse salt from a high concentration liquid. The zeolite membrane displayed poor separation performance when in situ deposition process was carried out for 3 h. Thus, it can be assumed that synthesis time ranging from 3 h to 6 h was not sufficient to develop full-fledged zeolites, as support by the XRD analysis in Fig. 9.

The internal concentration gradient (ICP) is the common phenomenon occurred in FO process. This phenomenon is undesirable as it will reduce the fluxes over a long period of membrane operation. The concentration polarization effect could be measured by calculating the structure parameter (S) of zeolite membrane. An increase in S-value indicated that a significant effect of ICP in the FO process. The S values of zeolite membranes were tabulated in Table 5. It was found that the S-value was small and comparable to the traditional FO membranes that synthesized on porous polymeric supporting layers [22]. The S-value for zeolite membrane prepared for 24 h increased, which can be correlated to the thick and dense layer of zeolite membrane on glass hollow fiber, in Fig. 12. The S-values for zeolite membranes prepared for 6, 12 and 18 h were considered low, which indicated an insignificant effect of the concentration polarization during FO process.

Table 6
Comparison between zeolite membranes in forward osmosis application.

Zeolite Loading (wt. %)	Water Fluxes (L m^{-2}h^{-1})	Reverse solute fluxes (kg m^{-2}h^{-1})	Draw concentration (ppm)	References
[a]0.5	72.0	0.05	100,000	This work
[b]0.4	30.0	0.02	58,400	[40]
[c]0.5	55.0	0.16	47,888	[41]
[d]10.0	2.5	–	–	[42]
[e]0.0	13.2	0.0017	40,000	[43]

[a] Zeolite growth on glass hollow fiber using hydrothermal method.
[b] Zeolite dispersed into the trimesoyl chloride (TMC) with n-hexane solution by ultrasonication on the polysulfone (PSf) supports.
[c] Zeolite mixed into the poly-4-formylstyrene (PSfN) substrates.
[d] Zeolite blended into mixture of polyvinylidene fluoride (PVDF)/ polyvinylpyrrolidone (PVP).
[e] Aquaporin in hollow fiber membrane modules.

The separation performance of zeolite membranes prepared in this work in forward osmosis applications was compared with various studies, as shown in Table 6. The zeolite membrane prepared using a reactant concentration of 0.66 M and deposition time of 18 h had a water flux of 72 L. m^{-2} h^{-1} and reverse solute of 0.05 kg m^{-2} h^{-1}. In comparison to Ma et. al's work [40], the zeolite membrane prepared in this study showed a higher water flux, possibly due to the peculiar properties of zeolite itself. Nevertheless, the membrane still allowed low reverse solute. In this work, high concentrations of draw solution was used (100,000 ppm) to evaluate the performance of the zeolite, different from other works that used lower concentration ranging from 40,000 to 60,000 ppm, as shown in Table 6. This justifies the reason of

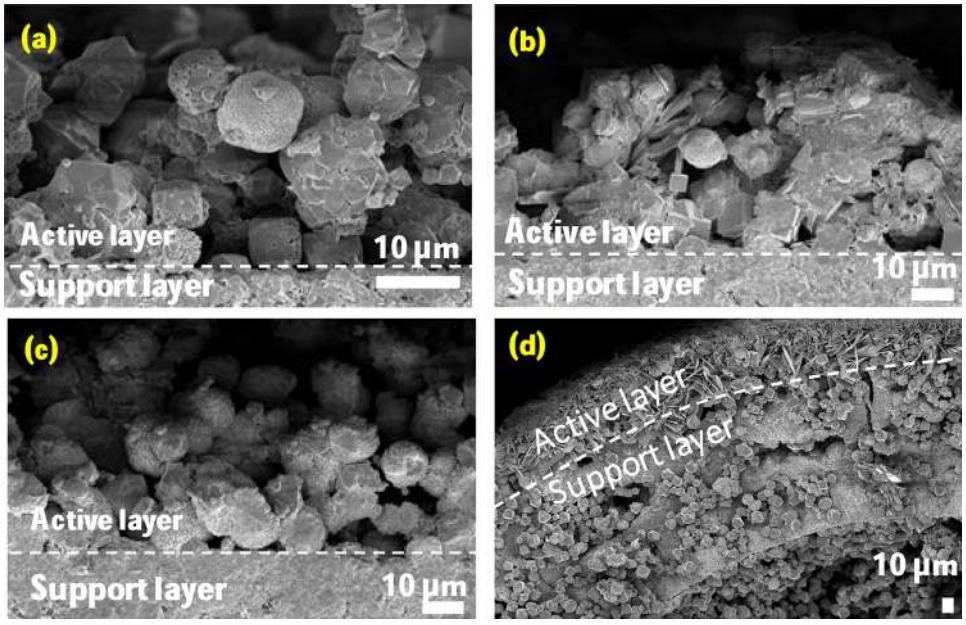

Fig. 12. Cross-sectional images of the zeolite membranes prepared for (a) 6 h, (b) 12 h, (c) 18 h and (d) 24 h at synthesis temperature of 120 °C.

slightly high reverse solute reported in this work, as the salt may leeched into feed flow during FO process. Nevertheless, zeolite membrane on glass hollow fiber still cannot match the performance of aquaporin membrane in FO. This phenomenon can be associated with grain boundaries (which is a type of defect for crystalline materials) of zeolite membrane that may allow considerable amount of salt to migrate into feed flow, causing significant reverse solute [37]. This case is irrelevant to polymeric membrane that possesses continuous polymer phase.

4. Conclusion

The effects of reactant concentrations and synthesis periods on in situ deposition of zeolite membranes on glass hollow fibers were studied. XRD analysis confirmed the presence of the zeolite phase when the reactant concentration of 0.66 M and synthesis period ranging from 12 to 24 h were applied during the deposition process. When the synthesis period ranging from 12 to 18 h was used, zeolite particles were found to have significant BET surface areas. The separation performances of zeolite membranes were studied using the forward osmosis system. The reactant concentration of 0.66 M (24 h reaction period) enabled the separation process to occur which gave a positive water flux of 4.50 L $m^{-2}h^{-1}$ with reverse solute of 0.05 kg $m^{-2}h^{-1}$. When in situ deposition time was reduced to 12 h and 18 h, water fluxes increased to 62.25 and 71.92 L m^{-2} h^{-1}, respectively. Reverse solutes for zeolite membranes deposited on glass follow fiber prepared for 12 h and 18 h were 0.11 kg m^{-2} h^{-1} and 0.05 kg m^{-2} h^{-1}, respectively. Interestingly, both samples were shown to have significant surface area and porosity, enabling the zeolite membranes to facilitate the diffusion of water through its framework. The separation performances of zeolite membranes prepared in this work were comparable to other studies in forward osmosis applications.

Acknowledgements

The authors gratefully acknowledge the financial support from various parties, namely, the Islamic Educational, Scientific and Cultural Organization (ISESCO) (*R.J130000.7351.4B368*) Malaysia Ministry of Higher Education (MOHE) through FRGS (*0.J130000.7823.4F947*), the Higher Institution Centre of Excellence (HICoE) Research Grant (R.J090301.7846.4J176), and Universiti Teknologi Malaysia (UTM) through the Research University grant (Q.J130000.2446.04G30, Q.J130000.3551.05G77, Q.J130000.2523.19H79). Appreciation also goes to UTM Research Management Centre for both financial and technical supports.

References

[1] A.D. Khawaji, I.K. Kutubkhanah, J. Wie, Advances in seawater desalination technologies, Desalination 221 (2008) 47–69, https://doi.org/10.1016/j.desal.2007.01.067.
[2] M. Obaid, Z. Ghori, O. Fadali, K. Khalil, A.A. Almajid, N.A.M. Barakat, Amorphous SiO 2 NPs- incorporated Poly (vinylidene fluoride) electrospun nanofiber membrane for high flux forward osmosis desalination, ACS App. Mater. Lett. (2015), https://doi.org/10.1021/acsami.5b09945.
[3] M. Ghanbari, D. Emadzadeh, W.J. Lau, H. Riazi, D. Almasi, A.F. Ismail, Minimizing structural parameter of thin fi lm composite forward osmosis membranes using polysulfone / halloysite nanotubes as membrane substrates, Desalination 377 (2016) 152–162, https://doi.org/10.1016/j.desal.2015.09.019.
[4] G. Amy, N. Ghaffour, Z. Li, L. Francis, R. Valladares, T. Missimer, S. Lattemann, Membrane-based seawater desalination: present and future prospects, Desalination 401 (2017) 16–21, https://doi.org/10.1016/j.desal.2016.10.002.
[5] D.L. Shaffer, J.R. Werber, H. Jaramillo, S. Lin, M. Elimelech, Forward osmosis: where are we now? Desalination 356 (2015) 271–284, https://doi.org/10.1016/j.desal.2014.10.031.
[6] L. Wan, C. Zhou, K. Xu, B. Feng, A. Huang, Synthesis of highly stable UiO-66-NH 2 membranes with high ions rejection for seawater desalination, Microporous Mesoporous Mater. 252 (2017) 207–213, https://doi.org/10.1016/j.micromeso.2017.06.025.
[7] U. Mueller, G. Biwer, G. Baldauf, Ceramic Membranes for Water Treatment, (2010), pp. 987–994, https://doi.org/10.2166/ws.2010.536.
[8] V. Dalvi, Y. Pan, C. Staudt, T. Shung, Influential effects of nanoparticles, solvent and surfactant treatments on thin fi lm nanocomposite (TFN) membranes for seawater desalination, Desalination 420 (2017) 216–225, https://doi.org/10.1016/j.desal.2017.07.016.
[9] S.H. Jamali, T.J.H. Vlugt, L. Lin, Atomistic Understanding of Zeolite Nanosheets for Water Desalination, (2017), https://doi.org/10.1021/acs.jpcc.7b00214.
[10] S. Alfaro, C. Rodríguez, M.A. Valenzuela, P. Bosch, Aging time effect on the synthesis of small crystal LTA zeolites in the absence of organic template, Mater. Lett. 61 (2007) 4655–4658, https://doi.org/10.1016/j.matlet.2007.03.009.
[11] M. Safarpour, V. Vatanpour, A. Khataee, H. Zarrabi, High flux and fouling resistant reverse osmosis membrane modi fi ed with plasma treated natural zeolite, Desalination 411 (2017) 89–100, https://doi.org/10.1016/j.desal.2017.02.012.
[12] L. Li, N. Liu, B. Mcpherson, R. Lee, Influence of counter ions on the reverse osmosis through MFI zeolite membranes: implications for produced water desalination, Desalination 228 (2008) 217–225, https://doi.org/10.1016/j.desal.2007.10.010.
[13] Y.T. and N.S.-I. Kumakiri I., Application of a zeolite A membrane to reverse osmosis process.pdf, (n.d.). doi:https://doi.org/10.1252/jcej.33.333.
[14] K. Aoki, K. Kusakabe, S. Morooka, Gas permeation properties of A-type zeolite membrane formed on porous substrate by hydrothermal synthesis, J. Memb. Sci. 141 (1998) 197–205.
[15] H. Chen, J. Wydra, X. Zhang, P. Lee, Z. Wang, W. Fan, M. Tsapatsis, Hydrothermal Synthesis of Zeolites With Three-dimensionally Ordered Mesoporous-imprinted Structure, (2011), pp. 12390–12393.
[16] W. Dong, Y. Long, Preparation of an MFI-type zeolite membrane on a porous glass disc by substrate self-transformation, Chem. Commun. 2 (2000) 1067–1068, https://doi.org/10.1039/b001814g.
[17] M. Kukizaki, Large-scale production of alkali-resistant Shirasu Porous Glass (SPG) membranes: influence of ZrO_2 addition on crystallization and phase separation in Na_2O–CaO–Al_2O_3–B_2O_3–SiO_2 glasses; and alkali durability and pore morphology of the membranes, J. Memb. Sci. 360 (2010) 426–435, https://doi.org/10.1016/j.memsci.2010.05.042.
[18] S. Sukas, R.M. Tiggelaar, G. Desmet, H.J.G.E. Gardeniers, Fabrication of integrated porous glass for microfluidic applications, Lab Chip 13 (2013) 3061–3069, https://doi.org/10.1039/c3lc41311j.
[19] S. Nurfatin, N. Mohd, M.A. Rahman, A.F. Ismail, M.H.D. Othman, J. Jaafar, Preparation and characterization of glass hollow fiber membrane for water purification applications, Environ. Sci. Pollut. Res. 24 (2017) 15918–15928, https://doi.org/10.1007/s11356-017-9405-7.
[20] J.R. McCutcheon, M. Elimelech, Influence of concentrative and dilutive internal concentration polarization on flux behavior in forward osmosis, J. Memb. Sci. 284 (2006) 237–247, https://doi.org/10.1016/j.memsci.2006.07.049.
[21] N. Abdullah, M.H. Tajuddin, N. Yusof, Forward Osmosis (FO) for Removal of Heavy Metals, Elsevier Inc., 2019, https://doi.org/10.1016/B978-0-12-813902-8.00010-1.
[22] X. Zhao, C. Liu, Efficient removal of heavy metal ions based on the optimized dissolution- diffusion- flow forward osmosis process, Chem. Eng. J. 334 (2018) 1128–1134, https://doi.org/10.1016/j.cej.2017.11.063.
[23] W.A. Phillip, J.D. Schiffman, M. Elimelech, High Performance Thin-Film Membrane, 44 (2010), pp. 3812–3818, https://doi.org/10.1021/es1002555.
[24] S. Nurfatin, N. Mohd, M. Zahir, M. Pauzi, N. Mu, N. Muhamad, M.A. Rahman, Preparation, characterization and performance evaluation of supported zeolite on porous glass hollow fiber for desalination application, Arab. J. Chem. (2018), https://doi.org/10.1016/j.arabjc.2018.11.015.
[25] C. Xia, S. Zha, W. Yang, R. Peng, D. Peng, Preparation of yttria stabilized zirconia membranes on porous substrates by a dip-coating process, Solid State Ion. 133 (2000) 287–294.
[26] S. Hussain, S. Yoshimitsu, U. Suzana, Y. Katsuki, Q. Mahmood, A. Ali, Nano-Structured Porous Yttria-stabilized Zirconia Membrane for High-temperature CO 2 Capture From H 2 / CO 2 Mixture, (2016), pp. 4763–4774, https://doi.org/10.1007/s13369-016-2193-4.
[27] P. Taylor, Y. Gu, K. Kusakabe, S. Morooka, Effect of chelating agent 1, 5-diaminopentane on the microstructures of sol-gel derived zirconia membranes, Sep. Sci. Technol. 36 (002) (2019) 37–41, https://doi.org/10.1081/SS-100108356 16.
[28] L. Wondraczek, G. Gao, D. Möncke, T. Selvam, A. Kuhnt, W. Schwieger, D. Palles, E.I. Kamitsos, Thermal collapse of SAPO-34 molecular sieve towards a perfect glass, J. Non. Solids 360 (2013) 36–40, https://doi.org/10.1016/j.jnoncrysol.2012.10.001.
[29] K. Rodponthukwaji, C. Wattanakit, T. Yutthalekha, S. Assavapanumat, C. Warakulwit, W. Wannapakdee, J. Limtrakul, Catalytic upgrading of carboxylic acids as bio-oil models over hierarchical ZSM-5 obtained via an organosilane approach, RSC Adv. 7 (2017) 35581–35589, https://doi.org/10.1039/C7RA03890A.
[30] W. Schwieger, A.G. Machoke, T. Weissenberger, A. Inayat, T. Selvam, M. Klumpp, A. Inayat, Hierarchy concepts: classification and preparation strategies for zeolite containing materials with hierarchical porosity, Chem. Soc. Rev. 45 (2016) 3353–3376, https://doi.org/10.1039/C5CS00599J.
[31] W.C. Wong, L. Tak, Y. Au, C.T. Ariso, K.L. Yeung, Effects of synthesis parameters on the zeolite membrane growth, J. Memb. Sci. 191 (2001) 143–163.
[32] B.X. Xu, W. Yang, J. Liu, L. Lin, Synthesis of a High-Permeance NaA Zeolite Membrane by Microwave Heating, (2002), pp. 1998–2001.
[33] L. Yu, H. Wang, Y. Zhang, B. Zhang, J. Liu, Recent advances in halloysite nanotube derived composites for water treatment, Environ. Sci. Nano 3 (2016) 28–44, https://doi.org/10.1039/C5EN00149H.
[34] W. Zhao, B. Basnet, I.J. Kim, Carbon nanotube formation using zeolite template and applications, J. Adv. Ceram. 1 (2012) 179–193, https://doi.org/10.1007/s40145-012-0018-9.
[35] Y.C. Feng, Y. Meng, F.X. Li, Z.P. Lv, J.W. Xue, Synthesis of mesoporous LTA zeolites with large BET areas, J. Porous Mater. 20 (2013) 465–471, https://doi.org/10.1007/s10934-012-9617-7.

[36] M. Zahir Mohd Pauzi, N. Mu'ammar Mahpoz, N. Abdullah, M.A. Rahman, K. Hamimah Abas, A. Abd Aziz, M. Hasbullah Padzillah, M. Hafiz Dzarfan Othman, J. Jaafar, A. Fauzi Ismail, Feasibility study of CAU-1 deposited on alumina hollow fiber for desalination applications, Sep. Purif. Technol. 217 (2019) 247–257, https://doi.org/10.1016/j.seppur.2019.02.021.

[37] N. Mu, N. Abdullah, M. Zahir, M. Pauzi, M.A. Rahman, K.H. Abas, A.A. Aziz, M. Hafiz, D. Othman, J. Jaafar, A.F. Ismail, Synthesis and performance evaluation of zeolitic imidazolate framework-8 membranes deposited onto alumina hollow fiber for desalination, Desalination 36 (2019) 439–449, https://doi.org/10.1007/s11814-018-0214-6.

[38] K. Okamoto, H. Kita, K. Horii, Zeolite NaA membrane: preparation, single-gas permeation, and pervaporation and vapor permeation of Water/Organic liquid mixtures, Ind. Eng. Chem. Res. 40 (2001) 163–175, https://doi.org/10.1021/ie0006007.

[39] B. Bayati, A.A. Babaluo, R. Karimi, Hydrothermal synthesis of nanostructure NaA zeolite: the effect of synthesis parameters on zeolite seed size and crystallinity, J. Eur. Ceram. Soc. 28 (2008) 2653–2657, https://doi.org/10.1016/j.jeurceramsoc.2008.03.033.

[40] N. Ma, J. Wei, R. Liao, C.Y. Tang, Zeolite-polyamide thin film nanocomposite membranes: towards enhanced performance for forward osmosis, J. Memb. Sci. 405–406 (2012) 149–157, https://doi.org/10.1016/j.memsci.2012.03.002.

[41] N. Ma, J. Wei, S. Qi, Y. Zhao, Y. Gao, C.Y. Tang, Nanocomposite substrates for controlling internal concentration polarization in forward osmosis membranes, J. Memb. Sci. 441 (2013) 54–62, https://doi.org/10.1016/j.memsci.2013.04.004.

[42] F.U. Nigiz, Complete desalination of seawater using a novel polyvinylidene fluoride / zeolite membrane, Environ. Chem. Lett. 16 (2018) 553–559, https://doi.org/10.1007/s10311-017-0684-5.

[43] J. Ren, R. Mccutcheon, A new commercial biomimetic hollow fi ber membrane for forward osmosis, Desalination 442 (2018) 44–50, https://doi.org/10.1016/j.desal.2018.04.015.